Project no. 282688

ECLIPSE

Evaluating the **Cl**imate and Air Quality **Imp**acts of **S**hort-Liv**e**d Pollutants

Collaborative Project

Work programme: Climate forcing of non UnFCCC gases, aerosols and black carbon

Activity code: ENV.2011.1.1.2-2

Coordinator: Andreas Stohl, NILU - Norsk institutt for luftforskning

Start date of project: November 1st, 2011

Duration: 36 months

Deliverable D5.6 Paper on novel metrics submitted to peer reviewed journal

Due date of deliverable: project month 33

Actual submission date: project month 38

Organisation name of lead contractor for this deliverable: CICERO

Scientist responsible for this deliverable: Keith P Shine, UREAD

Revision Draft 1

Project co-funded by the European Commission within the Seventh Framework Programme (2007-2013)		
Dissemination Level		
PU	Public	
PP	Restricted to other programme participants (including the Commission Services)	X
RE	Restricted to a group specified by the consortium (including the Commission Services)	
CO	Confidential, only for members of the consortium (including the Commission Services)	

A possible emissions metric for changes in the global hydrological cycle

Keith P Shine[1,*], William Collins[1] and Jan S Fuglestvedt[2]

[1]Department of Meteorology, University of Reading, UK

[2]Center for International Climate and Environmental Research–Oslo, Oslo, Norway

[*]Corresponding author – email: k.p.shine@reading.ac.uk

To be submitted to Earth System Dynamics

Abstract

Improved understanding of the factors determining global precipitation response to climate change is used to explore an emissions metric (akin to the global warming potential (GWP) and global temperature-change potential (GTP)), which measures the effect of different emissions on global-mean precipitation relative to CO_2. The new index is named the Global Precipitation-change Potential (GPP). Since precipitation changes are highly variable in size and sign between different regions, global-mean precipitation change is not directly related to impact of climate change. Nevertheless, the new index broadly indicates the relative ability of different emissions to disturb the hydrological cycle. Results are reported for pulse (subscript P) and sustained (subscript S) emissions for selected long- and short-lived forcing agents using illustrative values of required parameters, a key one being the surface-atmosphere partitioning of radiative forcing. The GPP_P for N_2O significantly exceeds its GWP and GTP_P, because N_2O and CO_2 likely differ in their surface-atmosphere partitioning of forcing. For short-lived forcings, the GPP_P is similar to the GTP_P, but the GPP_S is opposite in sign to the GTP_S for black carbon emissions. The choice of CO_2 as a reference gas is problematic, especially for the GPP_S at short time horizons, because its size and sign are sensitive to uncertainties in its calculation. The new framework presents an additional perspective for comparing different forcings which is further down the cause-effect chain from emissions to impacts than most other physically-based metrics. However, there is more uncertainty in its quantification because few studies have presented results for the surface-atmosphere partitioning of different forcings. It is not proposed that the GPP could replace the GWP and GTP as a metric, but that it could be used in conjunction with these.

1. Introduction

Emissions of greenhouse gases, aerosols or species that influence aerosol or ozone formation can lead to climate change. There is utility in expressing the effect of emissions, in terms of their future impact on the climate system, on some kind of common scale. Most notably, the 100-year time-horizon global warming potential (GWP (100)) is used by the Kyoto Protocol to the United Nations' Framework Convention on Climate Change to place emissions of many relatively well-mixed non-CO_2 greenhouse gases on a so-called "CO_2-equivalent scale"; this is necessary for the type of multi-gas treaty that the Kyoto Protocol represents. . National emissions targets are often stated in terms of CO_2-equivalence using the GWP(100). Metrics such as the GWP can also be used for assessing possible mitigation strategies, for example in particular economic sectors, and can extend beyond the gases included in the Kyoto Protocol (see e.g., Fuglestvedt et al. 2010, Deuber et al. 2014).

The GWP characterises the radiative forcing (RF) in response to a pulse emission of a substance, integrated over some specified time horizon. It is normally expressed relative to the same quantity for an emission of CO_2. The GWP has enabled the operation of the Kyoto Protocol but has also been the subject of criticism for some applications (e.g., Myhre et al. (2014), Pierrehumbert (2014) and references therein). This is partly because the use of time-integrated RF does not clearly relate to an impact of climate change (such as temperature change) and also because it contains value judgements (particularly the choice of time horizon) that cannot be rigorously justified for any particular application (IPCC, 2014).

Metrics that extend beyond time-integrated forcing have also been proposed. The Global Temperature-change Potential (GTP) (e.g., Shine et al. 2007; Myhre et al. 2014) characterises the global-mean surface temperature change at some time after an emission. It may be more applicable to policies that aim to restrict temperature change below a given target level. The GTP is also subject to criticism and the need for value judgements when choosing time horizons. Nevertheless it (and its variants, such as the mean global temperature-change potential (e.g., Gillett and Matthews 2010, Deuber et al. 2014) and integrated temperature potential (e.g., Peters et al. 2011, Azar and Johansson, 2012) do at least extend to a parameter (temperature change) more obviously related to a climate change impact. Sterner et al. (2014) also recently presented a metric for sea-level rise. Metrics can be extended to the economic effects of an emission (for example the Global Cost Potential and Global Damage Potential), by relating the metrics to costs and damages (e.g., Johansson 2012) and in certain restrictive cases these can be shown to have equivalence to physically-based metrics such as the GWP and GTP (e.g., Tol et al. 2012). One difficulty in such approaches is that the economic damage has to be represented in a highly-idealised form, as some simple function of, for example, temperature change. Conventional physical metrics can also be judged in an economic context (e.g., Reisinger et al. 2012, Strefler et al. 2014)

Since the impact of climate change depends on more than just temperature change this paper explores a new metric that exploits advances in understanding as to how RF and temperature change relate to global precipitation change. Such a metric has the attraction that precipitation change, like the GTP, is an impact of climate change on human and natural systems.

However, in addition to the general difficulties in formulating metrics discussed above, precipitation change is much less amenable to a global representation than temperature change. Average surface temperature response to increased concentrations of greenhouse gases is largely the same sign over the whole planet, the temperature changes are coherent on large spatial scales, and climate models largely agree on the pattern of temperature change, if not the absolute size (e.g. Knutti and Sendláček 2012). By contrast, precipitation changes vary regionally in sign, are spatially much more variable and there is much less agreement between climate models on the patterns of response (e.g. Knutti and Sendláček 2012).

Nevertheless, for increased concentrations of well-mixed greenhouse gases, there is a general pattern of response embodied in the "the wet gets wetter and the dry gets drier" generalisation of the projected future change in the hydrological cycle (IPCC 2014), which is superimposed on a global-average increase in precipitation. We name the new metric the Global Precipitation-change Potential (GPP). Such a global-mean metric can be regarded as at least an indicator of the size of disturbance of the global hydrological cycle. At the very least, the work presented here has pedagogical value in illustrating the response of the global precipitation to an emission of a particular gas, aerosol or precursor, and for showing the interplay between the time-dependence of the RF and the surface temperature response (and how different climate forcing agents differ in this interplay).

Section 2 presents the simple conceptual model that is used to relate precipitation change to RF and temperature change. Section 3 presents some illustrative examples of the GPP and compares it with more conventional metrics (the GWP and GTP) drawing values of key constants from the literature, assuming pulse and sustained emissions of a gas. Section 4 explores some aspects of the uncertainty in characterising the GPP. Section 5 presents a discussion of future prospects for further developing the GPP.

2. Simple conceptual model

The simple conceptual model presented here originates from the analysis of simulated precipitation changes in response to increases in CO_2 presented by Mitchell et al. (1987). The conceptual model has been further developed more recently, and extended to both multi-model assessments and other climate forcing (and feedback) mechanisms (e.g. Andrews et al. 2010, Kvalevåg et al. 2013, Allan et al. 2014, Takahashi 2009).

The framework starts with an expression of the global-mean atmospheric energy budget, whereby the net emission of radiation by the atmosphere (i.e. the atmospheric radiative divergence (R_a), which is the sum of the emission of longwave radiation by the atmosphere minus the atmospheric absorption of longwave and shortwave radiation) is balanced by the input of surface sensible (*SH*) and latent (*LH*) heat fluxes so that

$$R_a = LH + SH \, . \qquad (1)$$

LH is directly related to the precipitation as, at the global-mean level, evaporation (and hence hence *LH* fluxes) and precipitation approximately balance.

In response to the imposition of an RF and subsequent changes in temperature, humidity and clouds, R_d will change. The latent heat change ΔLH can then be written

$$\Delta LH = \Delta R_d - \Delta SH \, . \qquad (2)$$

ΔLH in W m^{-2} can be converted to precipitation units of mm day^{-1} by multiplication by 0.034 (86400 seconds in a day divided by the latent heat of vaporisation, L (2.5 x 10^6 J kg^{-1} at 273.15 K)). There is some level of approximation in this conversion, as L is temperature dependent and some precipitation falls as snow rather than rain. The precipitation change could also be quoted in % of total global mean precipitation (about 2.6 mm day^{-1} (e.g. Adler et al., 2003))

ΔR_d has two components. First, the RF mechanism can directly influence R_d by changing the absorption of shortwave radiation and/or the emission and absorption of longwave radiation. The conventional top-of-atmosphere radiative forcing (*RF)* can be written as the sum of a surface component (RF_s) and an atmospheric component (RF_a). Following Andrews et al. (2010) we define a parameter f such that $RF_a = f\,RF$. The parameter f can be derived directly from *RF* calculations or else diagnosed from fixed-sea-surface-temperature climate model simulations (e.g. Andrews et al. 2010, Kvalevåg et al 2103); these have the advantage that they include rapid adjustments of, for example, clouds but also a disadvantage as the value of f is derived from regression analyses and so has a statistical uncertainty that is particularly large for small forcings. Second, the temperature change (and resulting changes in other radiatively-important components such as cloud and water vapour) in response to this RF contributes to ΔR_d. Climate model simulations indicate that this term varies approximately linearly with global-mean surface temperature T_s (e.g. Lambert and Webb, 2008, Previdi 2010, O'Gorman et al. 2012). These papers also indicate that while generally a smaller term, ΔSH has a similar dependency. Hence it is convenient to combine the feedback-related changes in R_d and *SH* into a single term and separate out the *RF* term. Equation (2) then becomes

$$\Delta LH = k\Delta T_s - fRF \, . \qquad (3)$$

Thorpe and Andrews (2014) show that this formulation does a reasonable job of simulating the precipitation changes from a large number of climate models. We will refer to two terms on the right-hand side as the "T-term" and "RF-term" respectively. Since the balance between these two terms will vary between climate forcing mechanisms (and as will be shown, they can act to either reinforce or oppose each other) the same ΔT_s from two different forcing mechanisms can result in a different ΔP.

Note the sign convention here. For the case of a positive *RF*, since k is positive, the effect of the T-term is to increase R_d as temperature increases – the increased radiative divergence then leads to a requirement for a greater latent heat flux (and hence an increase in precipitation) to maintain the tropospheric energy balance; this term provides the direct link between surface temperature change and precipitation change. If in this same case f (and hence RF_a) is positive, then the RF-term would oppose the T-term and act to suppress precipitation.

Physically, in this case, there is a positive RF_a and hence less "demand" for latent heating to balance the tropospheric energy budget.

As a simple example of the processes, consider the equilibrium response to a doubling of carbon dioxide, and take k = 2.2 W m^{-2} K^{-1} (consistent with the multi-model means in Previdi (2010) and Thorpe and Andrews (2014)), RF = 3.7 W m^{-2} (IPCC, 2014) and f = 0.8 (Andrews et al. 2010). Since in the equilibrium case $\Delta T_S = \lambda RF$, where λ is the climate sensitivity, and assuming f is independent of λ, Equation (3) becomes

$$\Delta LH = RF(k\lambda - f) \tag{4}$$

so that the offset between the T- and RF-terms depends strongly on λ. For a mid-range climate sensitivity of 0.8 K (W m^{-2})$^{-1}$, the T-term is 0.21 mm day^{-1}, the RF-term is 0.095 mm day^{-1} and hence the RF-term offsets about 50% of the precipitation change that would result from the T-term alone. Considering the IPCC (2014) "likely" range for λ, which is 0.4 to 1.2 K (W m^{-2})$^{-1}$, the RF-term offsets the T-term by about 90% for low λ and by 30% at high λ. The overall hydrological sensitivity ($\Delta P/\Delta T_S$) varies from 0.26 % K^{-1} to 2 % K^{-1} over this range.

To transform the understanding encapsulated in Equation (3) into a metric-based form, we consider first a pulse emission (indicated by a subscript P) of a unit mass of a gas at time t=0 and take the precipitation change a time H after the emission. Hence, this form of the metric is an "end-point metric": i.e. it gives the value at the time horizon, unlike the GWP, which is integrated over time, up to H. A time-integrated form of the GPP could also be formulated paralleling the time-integrated GTP discussed in the introduction.

GPP_P can be considered as either an absolute metric ($AGPP_P$), which is presented in units of mm day^{-1} kg^{-1} here, or else as relative to an emission of some reference gas (in which case it has no units, and is denoted as simply the GPP_P following the convention for GWPs and GTPs) . The T-term is k times the $AGTP_P$. Assuming for small perturbations that RF is linear in the concentration of the emitted species, x, and that the perturbation decays exponentially with time constant τ_x, then for a unit emission, the F term is given by $f_x A_x \exp(-H/\tau_x)$, where A is the specific RF (in W m^{-2} kg^{-1}) of the emitted species. Hence the absolute GPP (in mm day^{-1} kg^{-1}) is given by

$$AGPP_P^x(H) = 0.034(kAGTP_P^x(H) - f_x A_x \exp(-H/\tau_x)). \tag{5}$$

Although there is no necessity to present the GPP as relative to a reference gas, this does have some utility, and following the common practice for GWP and GTP, CO_2 is used as a reference gas here, although difficulties with this choice will be noted later. The GPP_P, relative to an equal mass emission of CO_2, would then be given by

$$GPP_P^x(H) = \frac{AGPP_P^x(H)}{AGPP_P^C(H)} \tag{6}$$

where the superscript C denotes CO_2.

Since a perturbation of CO_2 does not decay following a simple exponential, the calculation of $AGPP_P^C(H)$ is slightly more involved – see the Appendix for details.

The effect of a sustained emission of a unit mass of gas per year, from time t=0 can also be considered yielding a sustained GPP (subscript S). In this case, the (GTP_S) (see Shine et al. 2005) can be used for the T-term and the RF-term is now proportional to the time variation of the perturbation of the species to a step-perturbation so that the absolute GPP_S is given by

$$ASGPP_P^x(H) = 0.034(kAGTP_P^x(H) - f_x A_x \tau_x (1 - \exp(-H/\tau_x))) \quad (7)$$

with an analogous expression to Equation (6) for the SGPP relative to CO_2. The expression for $SGTP^C$ is given in the Appendix. Since a sustained emission can be considered to be equivalent to a succession of pulse emissions, GPP_S can be directly related to the GPP_P (see e.g., the Appendix of Berntsen et al. (2005)).

3. Illustrative values for the Global Precipitation-change Potential

In this section, illustrative calculations of the AGPP and GPP are presented. The calculations of GTP, gas lifetimes and A_x follow the methodology presented in Fuglestvedt et al. (2011). The calculation of GTP uses a simple representation of the surface temperature response, which depends on the climate sensitivity and rate of ocean heat uptake. The methodology here is follows the simple impulse-response approach in Boucher and Reddy (2008) (and was also used in Myhre et al. (2014) for GTP calculations), and is described in more detail in the Appendix, although sensitivity tests are presented in Section 4. Values of *f*, which describe the partitioning of the RF between surface and atmosphere are taken from Andrews et al. (2010) – these will likely be quite strongly model dependent, but for the purposes of illustration, they suffice. Some sensitivity tests are presented in Section 4.

3.1 Well-mixed greenhouse gases

Figure 1 shows the $AGPP_P$ for emissions of CO_2, CH_4 and N_2O, for the total and the RF and T terms individually, for a period up to 100 years after the pulse emission. In Andrews et al. (2010), *f* is larger for CO_2 (0.8) than for methane (0.5) and it is assumed here that *f* for N_2O is also 0.5. Hence the degree of offset between the RF- and T-terms is larger for CO_2. Figure 1(a) for CO_2 illustrates the general behaviour. For a pulse emission, the RF-term is maximised at the time of emission, as this is when the forcing is largest, and then decays as the perturbation decays. The T-term is dictated by the timescale of the response of the surface temperature to the forcing. The characteristic temperature response to a pulse forcing (e.g. Shine et al. 2005) is an initial increase in T, as the surface takes time to start to respond to the forcing, reaching a maximum, followed by a decrease in temperature that is controlled by the timescales of both the decay of the pulse and the temperature perturbation. For the first 5 years, the CO_2 precipitation response is negative as the negative RF term dominates, after which the T term dominates, but the total is approximately 50% of the T term. The long perturbation timescales mean that the effect on precipitation persists for more than 100 years after an emission, as does the competition between the T and RF terms.

Because N_2O is also long-lived, its $AGPP_P$ (Figure 1(b)) is qualitatively similar to CO_2 but the T-term dominates, because *f* is smaller. As CH_4 is much shorter lived, its behaviour is somewhat different. As the pulse, and the associated RF, has disappeared by about year 40, after this time, the $AGPP_P$ is essentially solely the T-term.

Figure 2 shows the GPP_P for the N_2O and CH_4; for comparison, the GTP_P is also shown. Note that the GPP_P plots start at H=20 years, as the time at which the different $AGPP_P$'s cross the zero axis differs slightly amongst the gases, and this results in a singularity in Eq. (2). For N_2O, its impact is at least 350 times greater than CO_2 on all timescales shown, and is about 30% more effective at modulating precipitation than temperature (as given by the GTP_P), compared to CO_2 because the RF term is less effective at muting the T-term for N_2O. For CH_4 the difference between the GPP_P and GTP_P is most marked at shorter time horizons, when the RF-term effects the GPP_P of methane most, but the GPP_P and the absolute difference with the GTP decline at longer time scales when it is entirely due to the difference between the $AGTP_P$ and APGPP for CO_2.

Table 1 presents the values of the GWP, GTP_P and GPP_P for H of 20 and 100 years; these time horizons are chosen for illustrative purposes, rather than being indicative that they have special significance, expect insofar as 100 years is used for the GWP within the Kyoto Protocol. For CH_4 this shows that for 20 years, the GPP_P is about double that of the GWP and GTP, although the time-integrated nature of the GWP_P means that this index is much higher than the GTP and GPP_P at 100 years (although as shown in Figure 1, the actual impact of the methane emissions is small at this H). The effectiveness of N_2O at changing precipitation (relative to CO_2) is significantly higher than the GWP and GTP_P at both values of H.

3.2 Short-lived species

The GPP is now illustrated for two short-lived species, sulphate and black carbon (BC) aerosols. For both cases, the direct RFs used in Fuglestvedt et al. (2011) are used. In terms of the surface-atmosphere partitioning of RF, these are two contrasting cases. For sulphate, Andrews et al. (2010) model results indicate an *f* value of -0.06, indicating that most of the top-of-the-atmosphere forcing reaches the surface, and RF_a is small. By contrast, for BC, *f* is 2.5; the RF_a is much greater than RF and the surface forcing is of opposite sign to RF and RF_a as the surface is deprived of energy, while the atmosphere gains energy. As will be discussed further in Section 4, there is considerable uncertainty in these values, especially for BC, where both RF and *f* depend significantly on the location of the BC. Nevertheless, the values used here suffice to illustrate a number of important points.

Figure 3 shows the $AGPP_P$ for both black carbon and sulphate. As both are very short-lived (weeks) compared to the greenhouse gases, their RF-term decays to zero within a year, and it is only the thermal inertia of the climate system that enables them to influence temperature beyond this time period. Hence, despite the radical difference in their values of *f* (2.5 for black carbon, -0.06 for sulphate) this has no impact in a pulse-based view beyond very short timescales. Because of this, in figure 4, which shows the GPP_P and GTP_P, the only difference between the GPP_P and GTP_P comes from the influence of the RF term on the $AGPP_S^C$, and

both short-lived species are, relative to CO_2, more effective at changing precipitation than temperature – this is also shown in Table 1.

An alternative perspective of the effect of sulphate and BC is provided for the sustained-emissions case. In this case, because the BC and sulphate perturbations persist, so does the influence of the RF-term on precipitation. Figure 5 shows the $AGPP_P$ for CO_2, BC and sulphate. For CO_2, the long-time scales of CO_2 perturbation mean that both the RF term and T term increase throughout the 100 year period shown. At short time-horizons, the RF-term dominates, leading to suppression of precipitation, but by about 15 years, the T-term starts to dominate, and the $AGPP_S$ becomes positive.

For BC, the impact of the large RF-term is dramatic. It is strongly negative and constant with time (because of the short-life time), while the T term is positive and increases until the temperature is almost in equilibrium with the RF. This mutes the impact of the RF term on the total, but the total nevertheless remains negative throughout. For sulphate, with its small value of *f*, the RF term is also small, but of the same sign as the T term, and hence the total effect is slightly larger than the T term.

Figure 6 shows the GPP_S, comparing it with the GTP_S. For sulphate, the two hardly differ, but they differ dramatically for black carbon – whilst both BC and CO_2 cause a warming, so that the GTP_S is positive, their impact on precipitation is opposite, and the GPP_S is negative.

Table 2 presents values of the GTP_S and GPP_S for H = 20 and 100 years, including the values for CH_4 and N_2O for completeness. The GPP_S values at 20 years are particularly influenced by the fact that the $AGPP_S$ for CO_2 is relatively small at this time, due to the almost cancellation between the T and RF terms. At both value of H, the GPP_S values are higher in magnitude than the corresponding GTP_S values.

4. Sensitivities and uncertainties

Two different sensitivities are explored here. First, the impulse-response model for surface temperature change used here (see beginning of Section 3) is a fit to output from experiments with one particular climate model with its own particular climate sensitivity. Olivié et al. (2012) present similar fits derived from 17 different climate models, or model variants, from the Coupled Model Intercomparison Project 3 database - the fits for the "gradual scenarios" shown in Table 5 of Olivié et al. (2012) are used here, along with the Boucher and Reddy (2008) fit used in Section 3. These fits are for models with a wide range of climate sensitivities (0.49 to 1.06 K $(W\ m^{-2})^{-1}$) and timescales of the fitted modes vary significantly amongst the models. Olivie and Peters (2013) used these fits to explore the sensitivity of the GTP to the impulse-response model for surface temperature change.

Table 3 shows the range of GTP_P and GPP_P values derived using these 18 different representations. Considering first the values for the absolute CO_2 it can be seen that the $AGTP_P$ is only moderately sensitive (about a factor of 2) to model choice. By contrast the $GPP_P(20)$ varies by over an order of magnitude and even the $GPP_P(100)$ varies by a factor of 3. This is because the T-term is highly sensitive to the model choice, whilst the RF-term is

independent, and hence the degree of compensation between these two terms varies amongst the impulse-response models. The GTP_P sensitivity is greatest for short-lived species (factors of 3 to 4) and this uncertainty is only slightly amplified for the GPP_P, because the dominance of the T-term removes one element of the sensitivity. By contrast, the longer-lived species are much more affected by uncertainty – for N_2O, the spread in the GTP_P values is only a few percent, but it is factors of 2 to 4 for the GPP_P, as both the numerator and denominator in the PGPP expression are impacted by compensations in the T- and RF-terms to different degrees.

The GPP_S(Table 4) is more problematical because even the sign of the CO_2 GPP_S is not well constrained at 20 years (roughly half of the impulse-response models yield a positive value and half a negative one, with two very close to zero) because of the differing degrees of compensation between the T- and RF-terms. In these circumstances, it becomes essentially pointless to compare the GPP_S values as they vary wildly from model to model (from -15000 to 26000 for the $GPP_S(20)$ for N_2O) and hence the $AGPP_S$ values are presented here. Even the $GPP_S(100)$ for CO_2 varies by over an order of magnitude.

The second sensitivity is the values of *f* used in the calculations. The values presented by Andrews et al. (2010) are replaced by those from Kvalevåg et al (2103) – in all cases, it is the larger perturbation values that are used from Kvalevåg et al (2103) as these give a clearer signal. For CO_2 *f* reduces from 0.8 to 0.6, for CH_4 (and, it is assumed for N_2O) it decreases from 0.5 to 0.35 and for sulphate it decreases from -0.06 to -0.4 (which implies much greater atmospheric absorption associated with sulphate forcing than found by Andrews et al. (2010). For BC, Kvalevåg et al (2103) present a range of values, appropriate for perturbations at different altitudes, which range from 6.2 to 13 (compared to the value of 2.5 used in Section 3).

Table 5 presents results for the GPP_P and GPP_S, and these should be compared with the appropriate columns in Tables 1 and 2 (the GWP, GTP_P and GTP_S values are unchanged when *f* is changed). For the GPP_P (10-20%) the changes are rather modest, for CH_4 and N_2O; these depend on the absolute values of CH_4, N_2O and CO_2 and the changes in the 2 compensate to some extent. For BC and sulphate, changes are entirely dependent on the change in $AGPP_P^C$, as the change in *f* factor has no influence – changes are correspondingly larger (20-30%).

For the GPP_S, the $AGPP_S^C(20)$ is rather sensitive to the change in *f* because of the degree of compensation between the T- and RF-terms, and increases by a factor of 2. This is the dominant reason why the $GPP_S(20)$ for N_2O and CH_4 decrease by about a factor of 2. The changes at 100 years are much smaller, nearer 10%. The short-lived species are now affected by the change in *f*. Table 5 shows the effect on the sulphate $GPP_S(20)$ to be about a factor of 2, while the $GPP_S(100)$ is little affected. By contrast, the GPP_S for black carbon at both time horizons depends significantly on the altitude of the black carbon perturbation.

5. Discussion and Conclusions

This paper has used a simple but powerful conceptual model of the drivers of global-mean precipitation change in response to the imposition of a radiative forcing, to derive emission metrics. The GPP_P and GPP_S metrics illustrate the interplay between the two drivers (the atmospheric component of the radiative forcing, and the surface temperature change) for different forcings, at different time horizons, and for both pulse and sustained emission viewpoints.

It has been shown that N_2O emissions are relatively more important than CO_2 in their impact on precipitation than they are on temperature and time-integrated forcing. Further, for black carbon emissions, while they act to warm the climate system, they also act to reduce global-mean precipitation; while this has been clear from the modelling literature for some time, the present work shows how the perspective is different for pulse and sustained emissions. The reduction of precipitation is driven entirely by the radiative forcing component, and since, for pulse emissions of short-lived species this falls away on time scales of weeks, it is only apparent on longer time scales for the sustained perspective.

The evaluation of precipitation metrics assumes that the parameters required for the simple conceptual model are available, and in particular the partitioning of radiative forcing between surface and atmosphere. Only a rather limited number of model studies of this partitioning are currently available, and there are differences amongst these. The ongoing Precipitation Driver Response Model Intercomparison Project (PDRMIP) (http://cicero.uio.no/PDRMIP/) should provide important information of the degree of robustness of this partitioning amongst a range of climate models for a number of radiative forcing mechanisms.

It is not suggested that the new metrics could replace conventional emissions metrics such as the GWP and GTP in a climate agreement or emission trading context, but they do provide a useful additional perspective, and particularly help to emphasise where the impact on precipitation differs significantly from that on temperature or forcing. One difficulty in its application is that conventional metrics generally use CO_2 as a reference gas. For precipitation change, the forcing and surface temperature components oppose each other, which means that the effect of CO_2 emissions can be zero (at least in the global-mean) at short time horizons for both pulse and sustained emissions. This is clearly undesirable for a reference gas, and it has also been shown that this zero point is rather sensitive to the particular parameters used in its calculation. Hence the absolute metric may be a more instructive metric.

It has been stressed that use of global-mean precipitation change as a measure of impact has difficulties, because predicted future changes vary in sign from region to region – the global-mean is a small residual of these opposing more localised changes and hence it only gives rather general guidance on the effect of different drivers on the changing hydrological cycle. The approach could be enhanced to a more regional level of response by either using a simple pattern-scaling approach (whereby the pattern of predicted precipitation change scales with the global-mean) or, better, to derive a regional variation that accounts for the different

effects of the forcing and temperature response on precipitation change (Good et al. 2012). The patterns emerging from such an approach would likely vary significantly on which climate model was used to derive them. In addition, such patterns would be needed for all possible forcings.

For short-lived emissions, it is known that even global-mean metrics such as the GWP and GTP depend on the emission location (e.g., Fuglestvedt et al. 2010) – this will also be true for the precipitation metrics. Metrics can also be posed in terms of the regional response to regional emissions, such as in the regional Global Temperature Potential proposed by Shindell (2012) whereby a matrix is produced that characterises the effect of a emissions in a set of given regions on the temperature change in a set of given regions. Regional versions of the GPP could also be derived, and it is likely that the regional variation of the response would be even larger for precipitation change than temperature change.

In spite of the difficulties in quantifying the precipitation metrics, given current understanding, the framework presented here adds a useful extra dimension to simple tools that are currently available for assessing the impact of emissions of different gases and particulates.

Acknowledgements: We acknowledge funding from the European Commission, under the ECLIPSE (Evaluating the Climate and Air Quality Impacts of Short-Lived Pollutants) Project (Grant Agreement 282688) and thank other ECLIPSE partners for their encouragement and input to this work.

Appendix

The impulse response function, *R(t)*, for a pulse emission of CO_2 is assumed to be of the form

$$R(t) = a_o + \sum_i a_i \exp\left(-\frac{t}{\alpha_i}\right) \qquad \text{(A1)}$$

where the parameters are the same as those in Fuglestvedt et al. (2011), with a_o=0.217, a_1=0.259, a_2=0.338, a_4=0.186 and α_1= 172.9 years, α_2= 18.51 years and α_3= 1.186 years.

The impulse response function for global-mean surface temperature is taken from Boucher and Reddy (2008) and is of the form

$$R(t) = \sum_i \frac{c_i}{d_i} \exp\left(-\frac{t}{d_i}\right) \qquad \text{(A2)}$$

with c_1=0.631 K (W m^{-2})$^{-1}$, c_2=0.429 K (W m^{-2})$^{-1}$ and d_1=8.4 years and d_2=409.5 years. The equilibrium climate sensitivity for a doubling of CO_2 for this impulse response function is 1.06 K.

Using Equation (A2), the $AGTP_P$ for a species with a specific RF A_i and a lifetime τ_i is given by

$$AGTP_P^x = A_i \tau_i \sum_{i=1}^{2} \frac{c_i}{\tau_i - d_i} (\exp(-t/\tau_i) - \exp(-t/d_i)) . \quad \text{(A3)}$$

Note that this equation would not apply in the case where $\tau_i = d_i$; the appropriate expression is given in Shine et al. (2005) for this case, which has to be modified for the two-term form of Equation (A2).

For the case of CO_2, where the decay of a pulse is given by Equation (A1), the $AGTP_P$ is given by

$$AGTP_P^C(t) = A_C (a_o \sum_{i=1}^{2} c_i (1 - \exp(-\frac{t}{d_i})) + \sum_{i=1}^{2} c_i \sum_{j=1}^{3} \frac{a_j \alpha_j}{\alpha_j - d_i} (\exp(-t/\alpha_j) - \exp(-t/d_i)) . \text{ (A4)}$$

For the case of CO_2, the exponential in the second term on the right-hand side of Equation (5) is replaced by Equation (A2).

For the GTP_S for non-CO_2 species is given by

$$AGTP_S^x = A_i \tau_i \left[\sum_{i=1}^{2} c_i (1 - \exp(-t/d_i) - \frac{\tau_i}{\tau_i - d_i} (\exp(-t/\tau_i) - \exp(-t/d_i))) \right] \quad \text{(A5)}$$

and again for the case where $\tau_i = d_i$, the appropriate expression is given in Shine et al. (2005), which has to be modified for the two-term form of Equation (A2).

For CO_2 the GTP_S is given by

$$ASGTP_s^C =$$

$$\sum_{i=1}^{2} A_C c_i [a_o (t - d_i (1 - \exp(-t/d_i))) + \sum_{j=1}^{3} \alpha_j a_j (1 - \exp(-t/d_i) - \frac{\alpha_j}{\alpha_j - d_i} (\exp(-t/\alpha_i) - \exp(-t/d_i)))] \quad \text{(A6)}$$

References

Adler, R. F., Huffman, G. J., Chang, A., Ferraro, R., Xie, P. P., Janowiak, J., et al. (2003). The version-2 global precipitation climatology project (GPCP) monthly precipitation analysis (1979-present). *Journal of Hydrometeorology, 4*(6), 1147-1167.

Allan, R. P., Liu, C. L., Zahn, M., Lavers, D. A., Koukouvagias, E., & Bodas-Salcedo, A. (2014). Physically Consistent Responses of the Global Atmospheric Hydrological Cycle in Models and Observations. *Surveys in Geophysics, 35*(3), 533-552.

Andrews, T., Forster, P. M., Boucher, O., Bellouin, N., & Jones, A. (2010). Precipitation, radiative forcing and global temperature change. *Geophysical Research Letters, 37*.

Azar, C., & Johansson, D. J. A. (2012). On the relationship between metrics to compare greenhouse gases the case of IGTP, GWP and SGTP. *Earth System Dynamics, 3*(2), 139-147.

Berntsen, T., Fuglestvedt, J., Joshi, M., Shine, K., Stuber, N., Ponater, M., et al. (2005). Response of climate to regional emissions of ozone precursors: sensitivities and warming potentials. *Tellus Series B-Chemical and Physical Meteorology, 57*(4), 283-304.

Boucher, O., & Reddy, M. S. (2008). Climate trade-off between black carbon and carbon dioxide emissions. *Energy Policy, 36*(1), 193-200.

Deuber, O., Luderer, G., & Sausen, R. (2014). CO2 equivalences for short-lived climate forcers. *Climatic Change, 122*(4), 651-664.

Fuglestvedt, J. S., Shine, K. P., Berntsen, T., Cook, J., Lee, D. S., Stenke, A., et al. (2010). Transport impacts on atmosphere and climate: Metrics. *Atmospheric Environment, 44*(37), 4648-4677.

Gillett, N. P., & Matthews, H. D. (2010). Accounting for carbon cycle feedbacks in a comparison of the global warming effects of greenhouse gases. *Environmental Research Letters, 5*(3).

Good, P., Ingram, W., Lambert, F. H., Lowe, J. A., Gregory, J. M., Webb, M. J., et al. (2012). A step-response approach for predicting and understanding non-linear precipitation changes. *Climate Dynamics, 39*(12), 2789-2803.

IPCC. (2013). *Climate Change 2013: The Physical Science Basis. Contribution of Working Group I to the Fifth Assessment Report of the Intergovernmental Panel on Climate Change*. Cambridge, United Kingdom and New York, NY, USA: Cambridge University Press.

Johansson, D. J. A. (2012). Economics- and physical-based metrics for comparing greenhouse gases. *Climatic Change, 110*(1-2), 123-141.

Knutti, R., & Sedlacek, J. (2013). Robustness and uncertainties in the new CMIP5 climate model projections. *Nature Climate Change, 3*(4), 369-373.

Kvalevag, M. M., Samset, B. H., & Myhre, G. (2013). Hydrological sensitivity to greenhouse gases and aerosols in a global climate model. *Geophysical Research Letters, 40*(7).

Lambert, F. H., & Webb, M. J. (2008). Dependency of global mean precipitation on surface temperature. *Geophysical Research Letters, 35*(16).

Mitchell, J. F. B., Wilson, C. A., & Cunnington, W. M. (1987). On CO_2 climate sensitivity and model dependence of results. *Quarterly Journal of the Royal Meteorological Society, 113*(475), 293-322.

Myhre, G., Shindell, D., Bréon, F.-M., Collins, W., Fuglestvedt, J., Huang, J., et al. (2013). Anthropogenic and Natural Radiative Forcing. In T. F. Stocker, D. Qin, G. K. Plattner, M. Tignor, S. K. Allen, J. Boschung, A. Nauels, Y. Xia, V. Bex & P. M. Midgley (Eds.), *Climate Change 2013: The Physical Science Basis. Contribution of Working Group I to the Fifth Assessment Report of the Intergovernmental Panel on*

Climate Change (pp. 659–740). Cambridge, United Kingdom and New York, NY, USA: Cambridge University Press.
O'Gorman, P. A., Allan, R. P., Byrne, M. P., & Previdi, M. (2012). Energetic Constraints on Precipitation Under Climate Change. *Surveys in Geophysics, 33*(3-4), 585-608.
Olivie, D. J. L., & Peters, G. P. (2013). Variation in emission metrics due to variation in CO2 and temperature impulse response functions. *Earth System Dynamics, 4*(2), 267-286.
Olivie, D. J. L., Peters, G. P., & Saint-Martin, D. (2012). Atmosphere Response Time Scales Estimated from AOGCM Experiments. *Journal of Climate, 25*(22), 7956-7972.
Peters, G. P., Aamaas, B., Berntsen, T., & Fuglestvedt, J. S. (2011). The integrated global temperature change potential (iGTP) and relationships between emission metrics. *Environmental Research Letters, 6*(4).
Pierrehumbert, R. T. (2014). Short-Lived Climate Pollution. *Annual Review of Earth and Planetary Sciences, 42*(1), 341-379.
Previdi, M. (2010). Radiative feedbacks on global precipitation. *Environmental Research Letters, 5*(2).
Reisinger, A., Havlik, P., Riahi, K., van Vliet, O., Obersteiner, M., & Herrero, M. (2013). Implications of alternative metrics for global mitigation costs and greenhouse gas emissions from agriculture. *Climatic Change, 117*(4), 677-690.
Shindell, D. T. (2012). Evaluation of the absolute regional temperature potential. *Atmospheric Chemistry and Physics, 12*(17), 7955-7960.
Shine, K., Fuglestvedt, J., Hailemariam, K., & Stuber, N. (2005). Alternatives to the global warming potential for comparing climate impacts of emissions of greenhouse gases. *Climatic Change, 68*(3), 281-302.
Shine, K. P., Berntsen, T. K., Fuglestvedt, J. S., Skeie, R. B., & Stuber, N. (2007). Comparing the climate effect of emissions of short- and long-lived climate agents. *Philosophical Transactions of the Royal Society a-Mathematical Physical and Engineering Sciences, 365*(1856), 1903-1914.
Sterner, E., Johansson, D. A., & Azar, C. (2014). Emission metrics and sea level rise. *Climatic Change, 127*(2), 335-351.
Strefler, J., Luderer, G., Aboumahboub, T., & Kriegler, E. (2014). Economic impacts of alternative greenhouse gas emission metrics: a model-based assessment. *Climatic Change, 125*(3-4), 319-331.
Takahashi, K. (2009). The Global Hydrological Cycle and Atmospheric Shortwave Absorption in Climate Models under CO2 Forcing. *Journal of Climate, 22*(21), 5667-5675.
Thorpe, L., & Andrews, T. (2014). The physical drivers of historical and 21st century global precipitation changes. *Environmental Research Letters, 9*(6).
Tol, R. S. J., Berntsen, T. K., O'Neill, B. C., Fuglestvedt, J. S., & Shine, K. P. (2012). A unifying framework for metrics for aggregating the climate effect of different emissions. *Environmental Research Letters, 7*(4).

Table 1: The absolute GWP (in 10^{-14} W m^{-2} kg^{-1} year), absolute GTP_P (in 10^{-16} K kg^{-1}) and absolute GPP_P (in 10^{-17} mm day^{-1} kg^{-1}) for a pulse emission of CO_2 and the GWP, GTP_P and GPP_P, relative to CO_2, for pulse emissions of 4 other species at time horizons of 20 and 100 years.

	GWP(20)	GWP(100)	$GTP_P(20)$	$GTP_P(100)$	$GPP_P(20)$	$GPP_P(100)$
Absolute CO_2	2.47	8.70	6.79	5.07	2.29	1.99
CH_4	72	25	57	3.8	101	7.2
N_2O	290	300	301	263	425	363
Sulphate	-140	-40	-41	-5.7	-91	-10.9
Black carbon	1600	450	460	64	1020	121

Table 2. The absolute GTP_S (in 10^{-14} K kg^{-1} year) and absolute GPP_S (in 10^{-15} mm day^{-1} kg^{-1} year) for a sustained emission of CO_2 and the GTP_S and GPP_S, relative to CO_2, for sustained emissions of 4 other species at time horizons of 20 and 100 years.

	$GTP_S(20)$	$GTP_S(100)$	$GPP_S(20)$	$GPP_S(100)$
Absolute CO_2	1.04	5.60	0.103	1.82
CH_4	80	27.8	311	43.6
N_2O	280	300	939	449
Sulphate	-201	-45.5	-1590	-109
Black carbon	2240	506	-15600	-667

Table 3: Spread in the $AGTP_P$ (in 10^{-16} K kg^{-1}) and $AGPP_P$ (in 10^{-17} mm day^{-1} kg^{-1}) for CO_2 and the GTP_P and GPP_P, relative to CO_2, for emissions of 4 other species at time horizons of 20 and 100 years, using alternative representations for the impulse-response function for temperature change

	$GTP_P(20)$	$GTP_P(100)$	$GPP_P(20)$	$GPP_P(100)$
Absolute CO_2	4.52 to 8.33	3.57 to 6.17	0.30 to 3.45	0.86 to 2.82
CH_4	43 to 61	2.6 to 6.5	85 to 322	5.3 to 19.3
N_2O	297 to 311	259 to 267	425 to 1290	333 to 703
Sulphate	-14 to -62	-3.9 to -9.4	-47 to -271	-7.2 to -27.9
Black carbon	128 to 692	39 to 105	524 to 3030	80.5 to 310

Table 4. The spread in $AGTP_S$ (in 10^{-14} K kg^{-1} year) and $AGPP_S$ (in 10^{-15} mm day^{-1} kg^{-1} year) for CO_2 and the GTP_S relative to CO_2 and $AGPP_S$ (in 10^{-15} mm day^{-1} kg^{-1} year) for emissions of 4 other species at time horizons of 20 and 100 years, using alternative representations for the impulse-response function for temperature change

	$GTP_S(20)$	$GTP_S(100)$	$AGPP_S(20)$	$AGPP_S(100)$
CO_2	0.67 to 1.29	3.39 to 6.88	-1.69 to 2.90	0.17 to 2.8
CH_4	76 to 81	27.1 to 28.9	1.17 to 4.68	0.32 to 1.06
N_2O	280 to 284	298 to 300	0.20 to 1.49	0.32 to 1.10
Sulphate	-170 to -207	-44.2 to -47.4	1.05 to 1.99	-1.20 to -2.40
Black carbon	1830 to 2310	492 to 528	1.19 to 2.24	-0.74 to -2.07

Table 5: The $AGPP_P$ (in 10^{-17} mm day^{-1} kg^{-1}) and $AGPP_S$ (in 10^{-15} mm day^{-1} kg^{-1} year) for a pulse emission of CO_2 and the GPP_P and GPP_S, relative to CO_2, for pulse 4 other species at time horizons of 20 and 100 years, but using the values of surface-atmosphere partitioning of radiative forcing from Kvalevåg et al. (2013). The range for black carbon is for different altitudes of the placement of black carbon.

	$GPP_P(20)$	$GPP_P(100)$	$GPP_S(20)$	$GPP_S(100)$
Absolute CO_2	2.99	2.44	0.271	2.41
CH_4	83	5.9	151	37.5
N_2O	382	330	490	390
Sulphate	-70	-8.9	-753	-98.8
Black Carbon	780	99	-24120 to -57610	-2540 to -6310

Figures

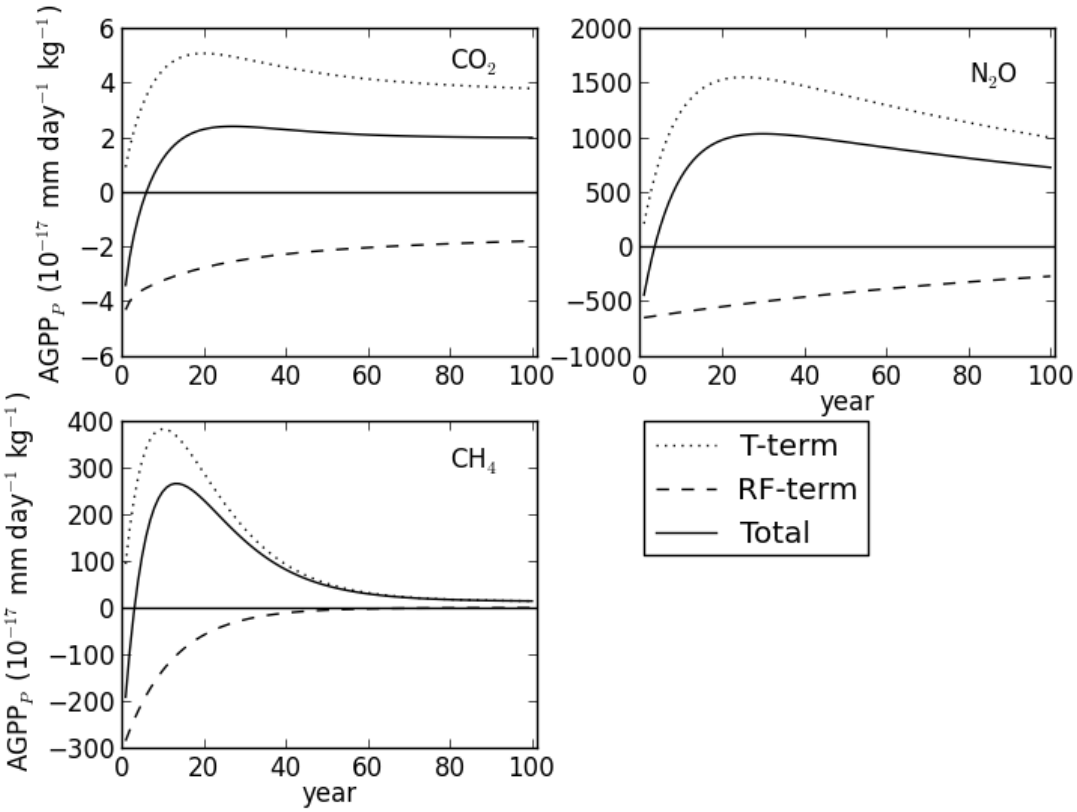

Figure 1: $AGPP_P$ for 1-kg pulse emissions of CO_2, N_2O and CH_4. The T-term and RF-term refer to the first and second terms on the right hand side of Eq. (5) respectively, and the Total term is the sum of these.

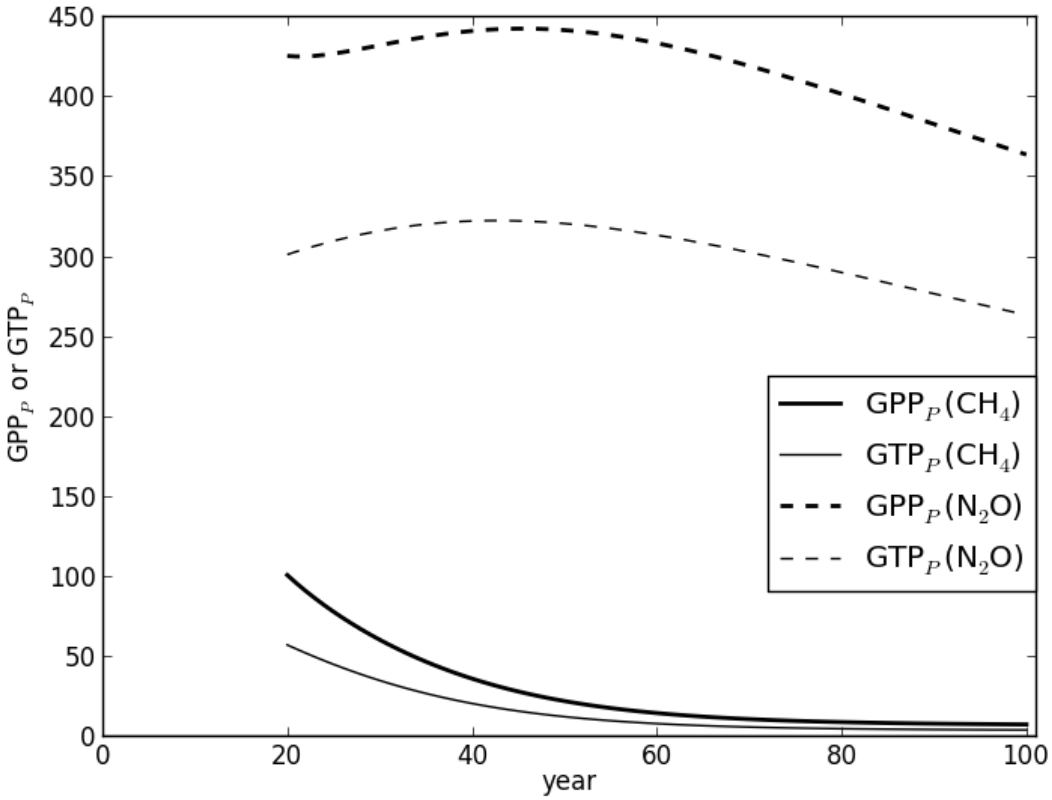

Figure 2: GPP_P (in bold) and GTP_P for 1-kg pulse emissions of N_2O and CH_4 relative to a 1-kg pulse emission of CO_2.

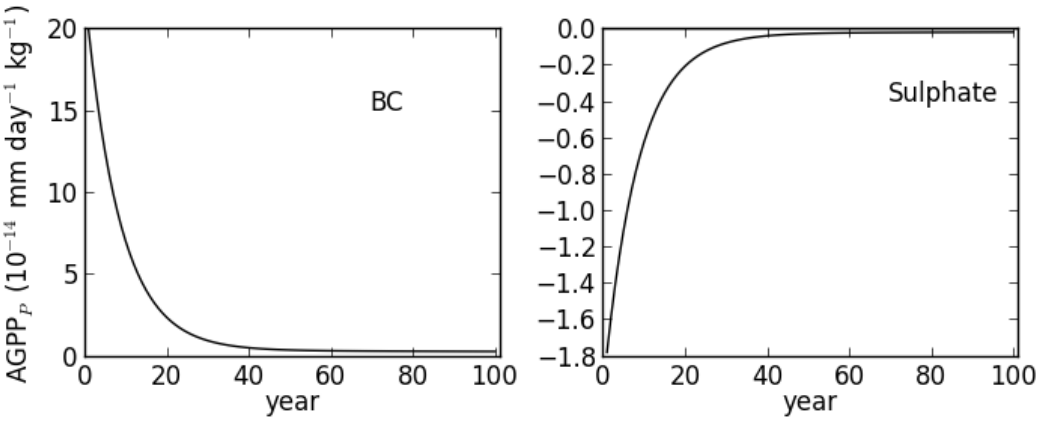

Figure 3: $AGPP_P$ for 1-kg pulse emissions of black carbon (BC) and sulphate. Note that the RF-term in Equation 5 is negligible for such short-lived gases, except at time horizons less than a few weeks, and only the total is shown.

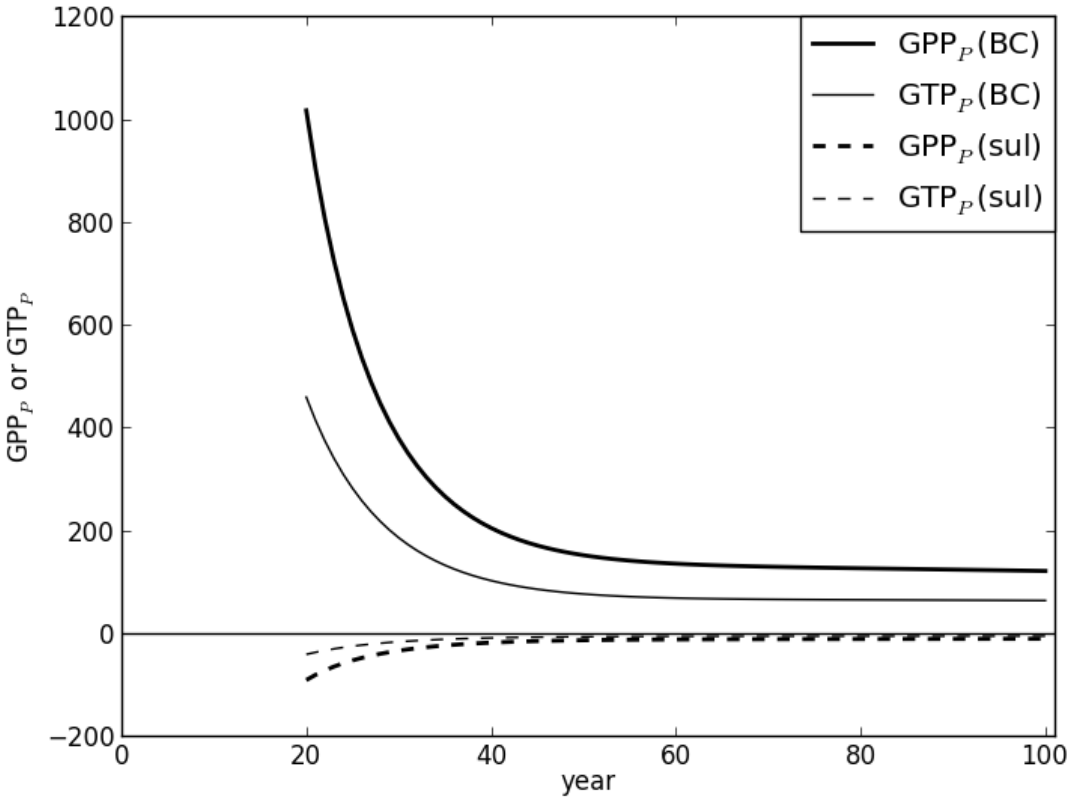

Figure 4: GPP_P (in bold) and GTP_P for 1-kg pulse emissions of BC and sulphate relative to a 1-kg pulse emission of CO_2.

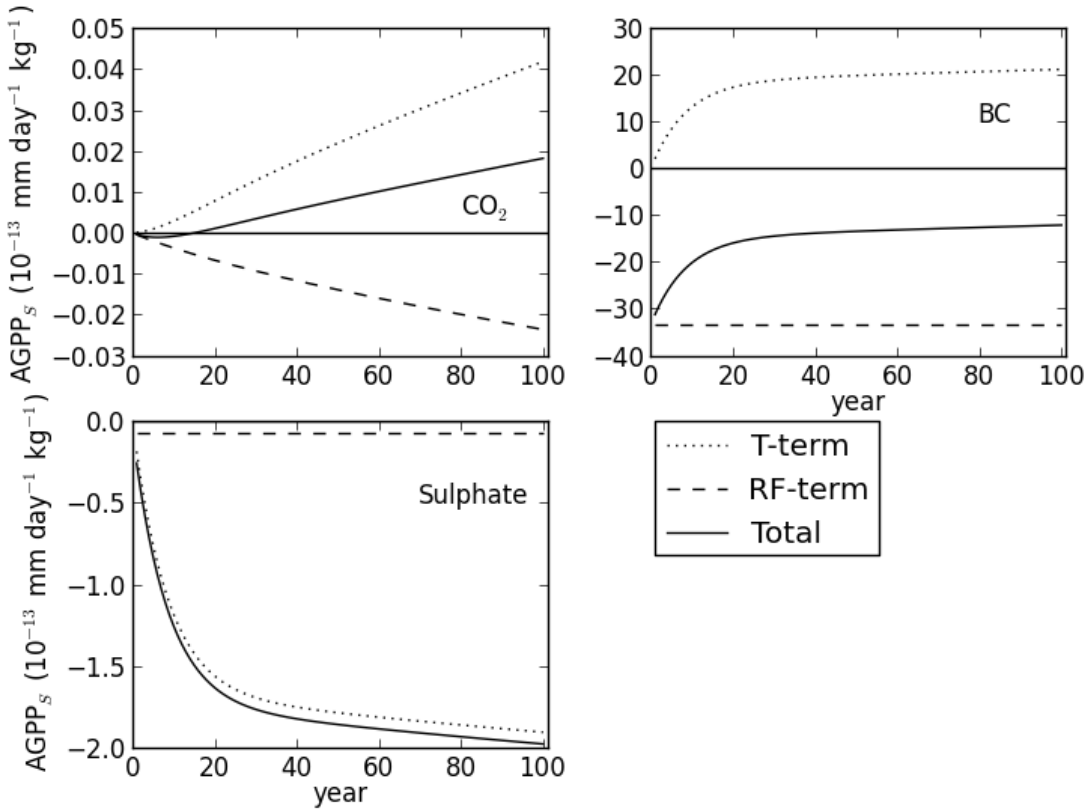

Figure 5: $AGPP_S$ for 1 kg year^{-1} sustained emissions of CO_2, BC and sulphate. The T-term and RF-term refer to the first and second terms on the right hand side of Eq. (7) respectively, and the Total term is the sum of these.

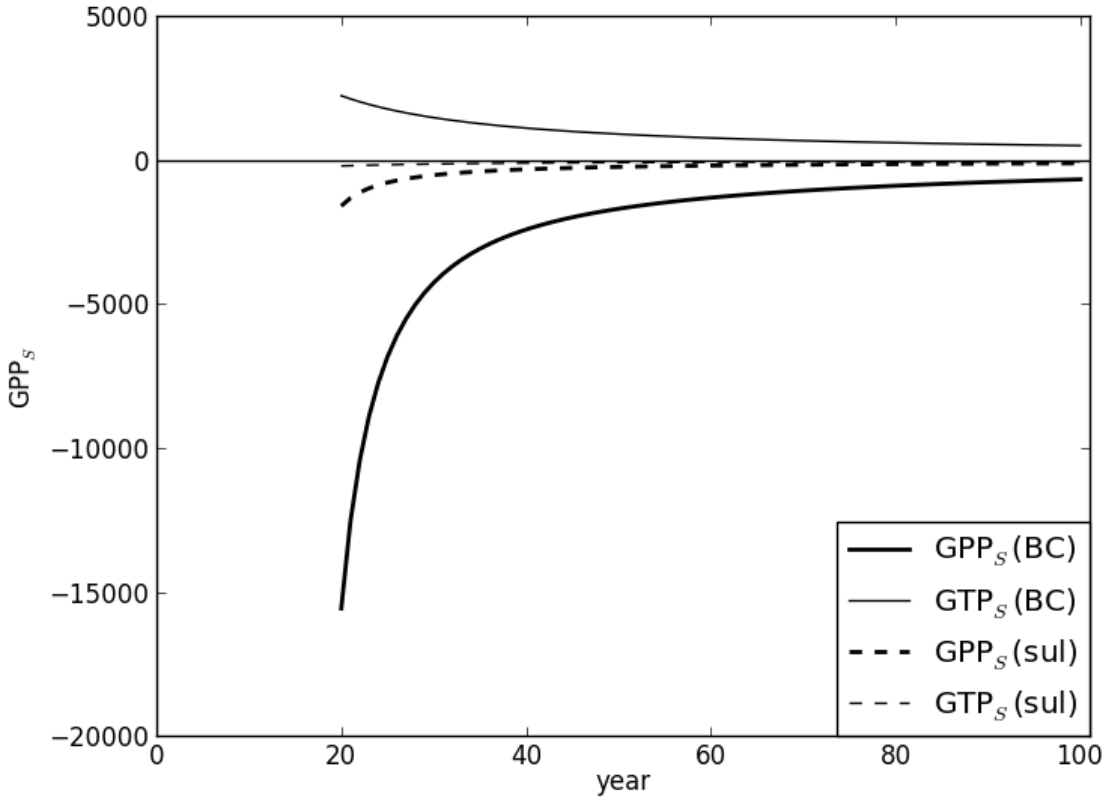

Figure 6. GPP_S (in bold) and GTP_S for 1 kg year^{-1} sustained emissions of BC and sulphate relative to a 1 kg year^{-1} sustained emission of CO_2.